

Advances in Digital Radiography: Physical Principles and System Overview¹

TEACHING POINTS

See last page

Markus Körner, MD • Christof H. Weber, MD • Stefan Wirth, MD
Klaus-Jürgen Pfeifer, MD • Maximilian F. Reiser, MD • Marcus Treitl, MD

During the past two decades, digital radiography has supplanted screen-film radiography in many radiology departments. Today, manufacturers provide a variety of digital imaging solutions based on various detector and readout technologies. Digital detectors allow implementation of a fully digital picture archiving and communication system, in which images are stored digitally and are available anytime. Image distribution in hospitals can now be achieved electronically by means of web-based technology with no risk of losing images. Other advantages of digital radiography include higher patient throughput, increased dose efficiency, and the greater dynamic range of digital detectors with possible reduction of radiation exposure to the patient. The future of radiography will be digital, and it behooves radiologists to be familiar with the technical principles, image quality criteria, and radiation exposure issues associated with the various digital radiography systems that are currently available.

©RSNA, 2007

Abbreviations: CCD = charge-coupled device, CR = computed radiography, DQE = detective quantum efficiency, DR = direct radiography, MTF = modulation transfer function, TFT = thin-film transistor

RadioGraphics 2007; 27:675-686 • Published online 10.1148/rg.273065075 • Content Code: **PH**

¹From the Department of Clinical Radiology, University Hospital Munich, Nussbaumstr 20, 80336 Munich, Germany. Presented as an education exhibit at the 2005 RSNA Annual Meeting. Received April 21, 2006; revision requested August 15 and received September 18; accepted September 18. All authors have no financial relationships to disclose. Address correspondence to M.K. (e-mail: markus.koerner@med.uni-muenchen.de).

©RSNA, 2007

Introduction

A systematic historical overview of the evolution of digital radiography is shown in Table 1. Experimental digital subtraction angiography was first described in 1977 by Kruger et al (1) and introduced into clinical use as the first digital imaging system in 1980 (2). For general radiography, x-ray images were first recorded digitally with cassette-based storage-phosphor image plates, which were also introduced in 1980 (3). The first DR system, which appeared in 1990, was the CCD slot-scan system. In 1994, investigations of the selenium drum DR system were published (4). The first flat-panel detector DR systems based on amorphous silicon (5) and amorphous selenium (6) were introduced in 1995. Gadolinium-oxide sulfide scintillators were introduced in 1997 (7) and have been used for portable flat-panel detectors since 2001 (8). The latest development in digital radiography is dynamic flat-panel detectors for digital fluoroscopy and angiography (9,10).

The most obvious advantage of digital detectors is that they allow implementation of a fully digital picture archiving and communication system, with images stored digitally and available anytime. Thus, distribution of images in hospitals can be achieved electronically by means of web-based technology without the risk of losing images. Other advantages include higher patient throughput, increased dose efficiency, and the greater dynamic range of digital detectors with possible reduction of x-ray exposure to the patient.

In this article, we provide an overview of the digital radiography systems currently available for general radiography. In so doing, we describe the physical principles of digital radiography and discuss and illustrate different systems in terms of detectors, image processing, image quality criteria, and radiation exposure issues. We also discuss future technologies and perspectives in digital radiography. Digital mammography has been reviewed in *RadioGraphics* elsewhere (11).

Physical Principles of Digital Radiography

The physical principles of digital radiography do not differ much from those of screen-film radiography (Fig 1). However, in contrast to screen-film radiography, in which the film serves as both detector and storage medium, digital detectors are used only to generate the digital image, which is then stored on a digital medium. Digital imaging

Table 1
Timetable of Developments in Digital Radiography

Year	Development
1977	Digital subtraction angiography
1980	Computed radiography (CR), storage phosphors
1987	Amorphous selenium-based image plates
1990	Charge-coupled device (CCD) slot-scan direct radiography (DR)
1994	Selenium drum DR
1995	Amorphous silicon-cesium iodide (scintillator) flat-panel detector
1995	Selenium-based flat-panel detector
1997	Gadolinium-based (scintillator) flat-panel detector
2001	Gadolinium-based (scintillator) portable flat-panel detector
2001	Dynamic flat-panel detector fluoroscopy-digital subtraction angiography

comprises four separate steps: generation, processing, archiving, and presentation of the image.

The digital detector is exposed to x-rays generated by a standard tube. Ultimately, the energy absorbed by the detector must be transformed into electrical charges, which are then recorded, digitized, and quantified into a gray scale that represents the amount of x-ray energy deposited at each digitization locus in the resultant digital image. After sampling, postprocessing software is needed for organizing the raw data into a clinically meaningful image.

After final image generation, images are sent to a digitized storage archive. A digital header file containing patient demographic information is linked to each image. Although it is possible to print digital images as hard-copy film, the advantages of digital radiography are not realized completely unless images are viewed digitally on a computer workstation. Digital images can be manipulated during viewing with functions like panning, zooming, inverting the gray scale, measuring distance and angle, and windowing. Image distribution over local area networks is possible. Digital images and associated reports can be linked to a digital patient record for enhanced access to diagnostic data.

Digital Detectors

Digital radiography can be divided into CR and DR (Fig 2).

CR systems use storage-phosphor image plates with a separate image readout process; DR is a way of converting x-rays into electrical charges by means of a direct readout process. DR systems can be further divided into direct and indirect conversion groups depending on the type of x-ray conversion used.

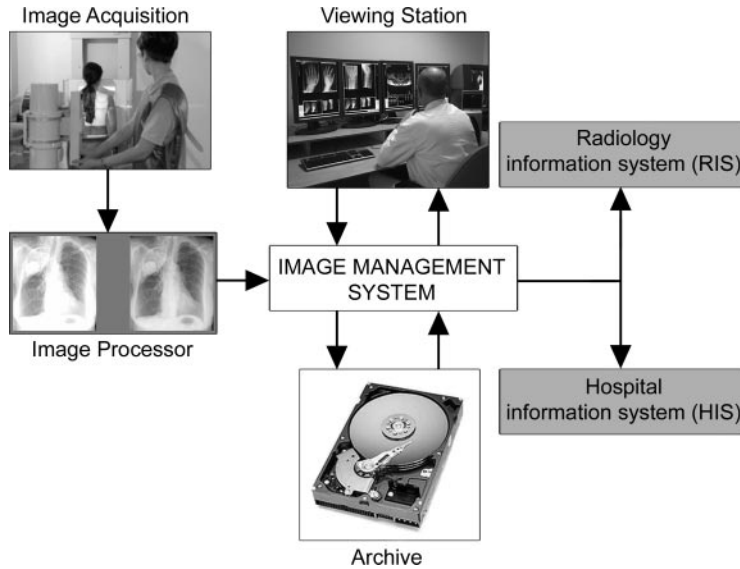


Figure 1. Chart illustrates a digital radiography system. After image exposure, the imaging data are digitally processed and stored in a digital archive. A centralized image management system is used for further distribution of the images to viewing stations, information systems, and electronic patient records.

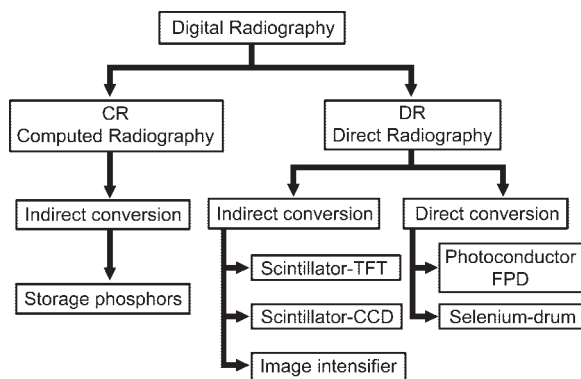


Figure 2. Chart provides a systematic overview of various types of digital detectors. *CCD* = charge-coupled device, *FPD* = flat-panel detector, *TFT* = thin-film transistor.

Computed Radiography

CR systems make use of image plates having a detective layer of photostimulable crystals that contain different halogenides such as bromide, chlorine, or iodine (eg, BaFBr:Eu²⁺). The phosphor crystals are usually cast into plates into resin material in an unstructured way (unstructured scintillators). Image plates replace the conventional films in the cassette.

The exposure process with storage-phosphor image plates is illustrated in Figure 3. During exposure, x-ray energy is absorbed and temporarily stored by these crystals by bringing electrons to higher energy levels. In this way, x-ray energy can be stored for several hours, depending on the specific physical properties of the phosphor crystals

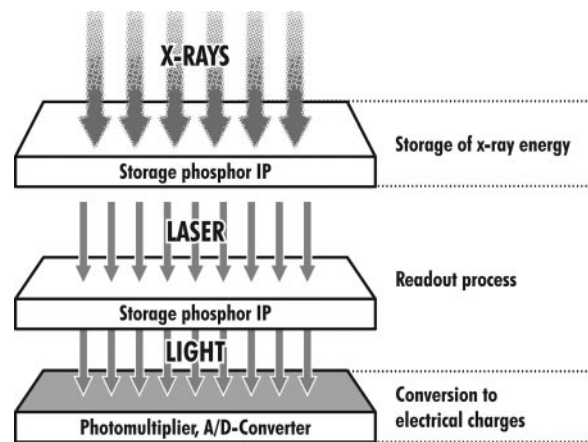


Figure 3. Drawing illustrates a CR system based on storage-phosphor image plates. Image generation is separated into two steps. First, the image plate (*IP*) is exposed to x-ray energy, part of which is stored within the detective layer of the plate. Second, the image plate is scanned with a laser beam, so that the stored energy is set free and light is emitted. An array of photomultipliers collects the light, which is converted into electrical charges by an analog-to-digital (*A/D*) converter.

used (12). However, the readout process should start immediately after exposure because the amount of stored energy decreases over time.

The readout process is a separate step that follows exposure of the image plate (Fig 3). When the detective layer is scanned pixel by pixel with a high-energy laser beam of a specific wave length (flying-spot scanner), stored energy is set free as emitted light having a wave length different from that of the laser beam. This light is collected by photodiodes and converted digitally into an image (12).

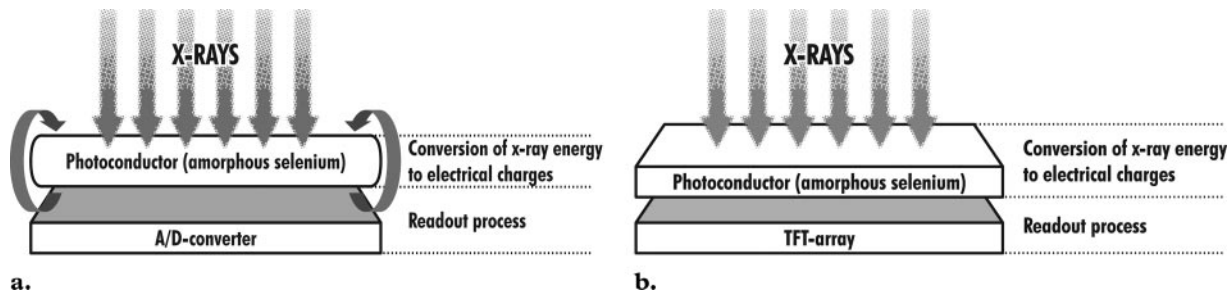


Figure 4. Amorphous selenium-based direct conversion DR systems. **(a)** Drawing illustrates a selenium drum-based system. A rotating selenium-dotted drum with a positive electrical surface charge is exposed to x-rays. Alteration of the charge pattern of the drum surface is proportional to the incident x-rays. The charge pattern is then converted into a digital image by an analog-to-digital (A/D) converter. **(b)** Drawing illustrates a selenium-based flat-panel detector system. Incident x-ray energy is directly converted into electrical charges within the fixed photoconductor layer and read out by a linked TFT array beneath the detective layer.

The whole readout process for a 14×17 -inch image plate takes about 30–40 seconds. Thus, a maximum workload of 90–120 image plates per hour is theoretically possible.

The advantages of storage-phosphor systems include a wide dynamic range, which leads to reduced rates of failed x-ray exposure. Because CR systems are cassette based, they can easily be integrated into existing radiographic devices, are highly mobile, and are easy to use for bedside examinations and immobile patients, making these systems flexible in routine clinical use. Furthermore, if a single image plate shows defects, it can easily be replaced by the radiographer with no need for specialized equipment or service personnel.

Spatial resolution with storage-phosphor image plates is usually lower than that with conventional screen-film combinations. However, several studies have shown that the diagnostic value of storage-phosphor radiography is at least equivalent to that of screen-film radiography (13–15). Still, compared with more modern digital detectors (eg, flat-panel detectors), storage-phosphor plates tend to be inferior in terms of image quality and diagnostic value, depending on the developmental stage of the storage-phosphor system being investigated (13,16–29).

Direct Radiography

Direct Conversion.—Direct conversion requires a photoconductor that converts x-ray photons into electrical charges by setting electrons free (30). Typical photoconductor materials include amorphous selenium, lead iodide, lead oxide, thallium bromide, and gadolinium compounds. The most commonly used element is selenium.

All of these elements have a high intrinsic spatial resolution (6). As a result, the pixel size, matrix, and spatial resolution of direct conversion detectors are not limited by the detector material itself, but only by the recording and readout devices used.

Selenium-based direct conversion DR systems are equipped with either a selenium drum or a flat-panel detector. In the former case, a rotating selenium-dotted drum, which has a positive electrical surface charge, is exposed to x-rays. During exposure, a charge pattern proportional to that of the incident x-rays is generated on the drum surface and is recorded during rotation by an analog-to-digital converter (Fig 4a) (30). Several clinical studies have confirmed that selenium drum detectors provide good image quality that is superior to that provided by screen-film or CR systems (4,13,16,17,31,32). However, because of their mechanical design, selenium drum detectors are dedicated thorax stand systems with no mobility at all.

A newer generation of direct conversion DR systems make use of selenium-based flat-panel detectors. These detectors make use of a layer of selenium with a corresponding underlying array of thin-film transistors (TFTs). The principle of converting x-rays into electrical charges is similar to that with the selenium drum, except that the charge pattern is recorded by the TFT array, which accumulates and stores the energy of the electrons (Fig 4b).

One advantage of these systems is greater clinical usefulness, since the detectors can be mounted on thorax stands and bucky tables. To date, there have been only a few clinical studies conducted with selenium-based flat-panel detectors. However, these studies indicate that the image quality provided by selenium-based flat-panel detectors is equivalent to that provided by other

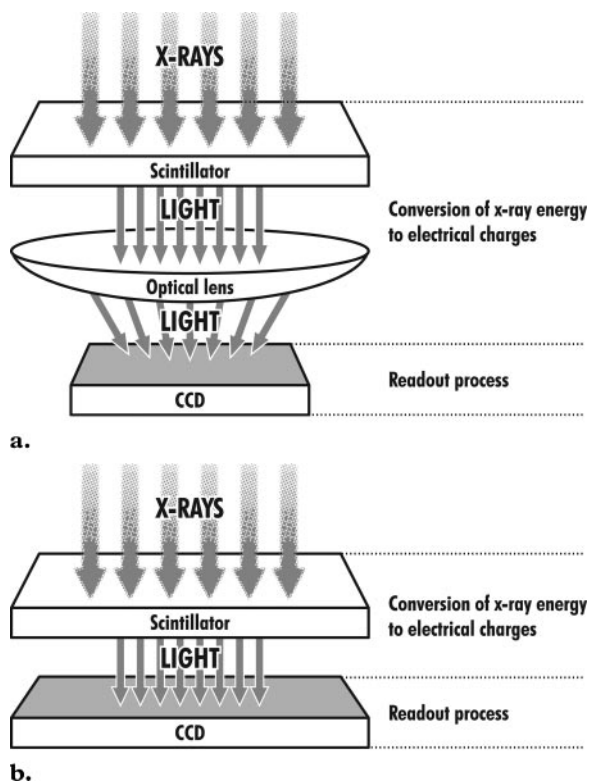


Figure 5. CCD-based indirect conversion DR system. (a) Drawing illustrates a lens-coupled CCD-based system. The incident x-ray energy is converted into light by a scintillator. The emitted light has to be bundled by an optical lens to fit the size of the CCD chip, which subsequently converts the light energy into electrical charges. (b) Drawing illustrates a slot-scan CCD-based system. The patient is scanned with a fan-shaped beam of x-rays. A simultaneously moving CCD detector of the same size collects the emitted light and converts the light energy into electrical charges.

flat-panel detectors and selenium drum detectors (17,32). Another promising clinical application of selenium-based flat-panel detectors is in the field of mammography (33).

Indirect Conversion with a CCD.—A CCD is a light-sensitive sensor for recording images that consists of an integrated circuit containing an array of linked or coupled capacitors. X-ray energy is converted into light by a scintillator such as Tl-doped cesium iodide. The amount of light emitted is then recorded by the CCD, and the light is converted into electrical charges.

Because the detector area cannot be larger than the CCD chip, it is necessary to combine several chips to create larger detector areas.

CCDs can be used for radiography as part of either a lens-coupled CCD system or a slot-scan CCD system. In lens-coupled CCD systems, an

array consisting of several CCD chips forms a detector area similar to that of a flat-panel detector. Optical lenses are needed to reduce the area of the projected light to fit the CCD array (Fig 5a). One drawback of the lens system is a decrease in the number of photons reaching the CCD, resulting in a lower signal-to-noise ratio and relatively low quantum efficiency (34).

Slot-scan CCD systems make use of a special x-ray tube with a tungsten anode. The patient is scanned with a collimated fan-shaped beam, which is linked to a simultaneously moving CCD detector array having a matching detector width (Fig 5b). The combination of a small collimated beam and a concordant detector reduces the impact of scattered radiation in the image, since much of this radiation will escape without detection. In addition, the relatively low quantum efficiency of slot-scan CCD systems, which is comparable to that of CR systems, can be offset by the resulting lower image noise (35). The exposure time to the patient is about 20 msec, and the readout process takes about 1.3 seconds (36). Because of the need for fixed installation, slot-scan CCD systems are dedicated to chest radiography, mammography, or dental radiography.

Studies dealing with CCD-based digital general radiography are rare. Phantom studies have been conducted to investigate slot-scan CCD systems and compare them with screen-film combinations (35,36) and various digital detectors (16,17,37). In all of these studies, CCD-based systems were comparable to flat-panel detectors in terms of image quality and allowed slightly superior low-contrast visualization. Clinical studies performed with slot-scan detectors are mainly concentrating on applications in mammography (11,38) and digital dental radiography.

The performance of lens-coupled CCD systems is somewhat inferior to that of slot-scan systems because of their technical principle (16,17), substantially lower quantum efficiency, and lower signal-to-noise ratio.

Indirect Conversion with a Flat-Panel Detector.—Indirect conversion DR systems are “sandwich” constructions consisting of a scintillator layer, an amorphous silicon photodiode circuitry layer, and a TFT array. When x-ray photons reach the scintillator, visible light proportional to the incident energy is emitted and then recorded by an array of photodiodes and converted to electrical charges. These charges are

then read out by a TFT array similar to that of direct conversion DR systems (Fig 6).

The scintillators usually consist of CsI or Gd_2O_2S . Gd_2O_2S crystals are cast into a binding material and are unstructured scintillators having a structure similar to that of storage phosphors (34).

The advantage of CsI-based scintillators is that the crystals can be shaped into 5–10- μm -wide needles, which can be arranged perpendicular to the surface of the detector. This structured array of scintillator needles reduces the diffusion of light within the scintillator layer (5,39,40). As a result, thicker scintillator layers can be used, thereby increasing the strength of the emitted light and leading to better optical properties and higher quantum efficiency (41).

One further advantage of flat-panel detectors is their small size, which allows integration into existing bucky tables or thorax stands. Because CsI-based flat-panel detectors are highly vulnerable to mechanical load because of their fine structure, these systems cannot be used outside of fixed installations and therefore lack mobility. Portable flat-panel detector systems make use of Gd_2O_2S -based scintillators, which are as resistant to mechanical stress as are storage phosphors (8,42, 43). Any defects that occur in the detector may cause a complete breakdown of the imaging system, making contingency imaging devices necessary.

Image generation with flat-panel detectors is almost a real-time process, with a time lapse between exposure and image display of less than 10 seconds. Consequently, these systems are highly productive, and more patients can be examined in the same amount of time than with other radiographic devices.

Many clinical studies have shown indirect conversion flat-panel detectors to provide superior image quality (39,40,44–47). Studies comparing indirect conversion flat-panel detectors with conventional screen-film combinations (18,21,22, 25,28,45,48–51), storage-phosphor image plates (17,18,20–27,29,52), or other digital detectors (16,17,31,37) have verified that flat-panel detectors offer the best image quality and low-contrast performance of all digital detectors and, so far, are superior to conventional screen-film combinations.

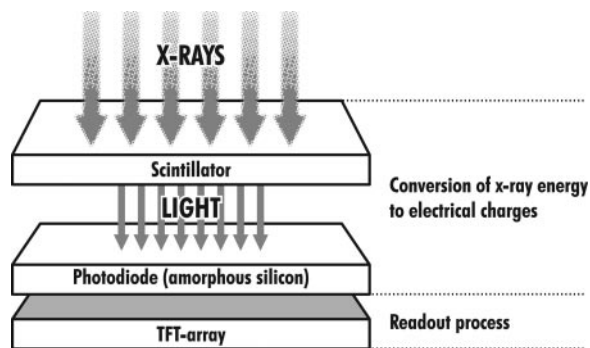


Figure 6. Drawing illustrates an amorphous silicon-based indirect conversion DR system. X-ray energy is converted into visible light in a scintillator layer. The emitted light is then converted into electrical charges by an array of silicon-based photodiodes and read out by a TFT array.

Image Processing

After exposure and readout, the raw imaging data must be processed for display on the computer (Fig 7). **Image processing is one of the key features of digital radiography, greatly influencing the way the image appears to the radiologist (53).**

Teaching Point

Although software products from several manufacturers use similar algorithms such as edge enhancement, noise reduction, and contrast enhancement to alter the appearance of the image, the resulting impressions may differ considerably.

Image processing is used to improve image quality by reducing noise, removing technical artifacts, and optimizing contrast for viewing. Spatial resolution (the capacity to define the extent or shape of features within an image sharply and clearly) cannot be influenced by the processing software because it is dependent on the technical variables of the detector (eg, pixel size). However, with optimization of other processing variables, lack of spatial resolution can be partially counteracted (53).

Altering processing features on digitally acquired images is not trivial. If one feature is being improved, others may be suppressed, so that unintended and unwanted masking of diagnostically relevant features may occur. Consequently, image processing must be optimized carefully for each digital radiography system. In addition, processing algorithms must be adapted to each anatomic region—meaning, for example, that different standards are required for lateral and posteroanterior chest radiography.

Image processing software is usually bundled with the detector and cannot be replaced by other software. In general, this arrangement allows processing algorithms to be optimized for a specific detector but does not rule out the possibility that use of a different processing software package might improve image quality even further.

A study by Prokop and Schaefer-Prokop (53) provides a more in-depth look at the technical possibilities of digital image processing.



Figure 7. Image postprocessing. The image on the far left represents the initially acquired raw data without any processing. The other three images have been digitally processed in different ways to illustrate the influence of various software tools on image appearance. Contrast enhancement (second image from left) makes anatomic structures more visible and distinguishable, contrast reduction (second image from right) results in smoothing of the structures, and edge enhancement (image on far right) provides sharper delineation of the fine structures of bones.

Table 2
Technical Features of Various Digital Radiography Systems

Feature	Type of System						
	Screen-Film	Storage-Phosphor	Lens-coupled CCD	Slot-Scan CCD	Direct FPD	Indirect FPD	Indirect FPD
Converter	Gd ₂ O ₂ S	BaSrFBr:Eu	Gd ₂ O ₂ S	CsI:TI	Selenium	Gd ₂ O ₂ S	CsI:TI
Readout	Film	Laser	CCD	CCD	Active selenium matrix	Active silicon matrix	Active silicon matrix
Detector size (in)	14 × 17	14 × 17	14 × 17	17 × 17	14 × 17	17 × 17	17 × 17
Pixel size (μm)	...	200	167	162	139	160	143
Matrix	...	1760 × 2140	2000 × 2500	2736 × 2736	2560 × 3072	2688 × 2688	3121 × 3121
Nyquist frequency (cycles/mm)	5	2.5	3.0	3.1	3.6	3.1	3.5
Dynamic range	1:30	1:40,000	>1:4000	1:10,000	>1:10,000	>1:10,000	>1:10,000

Note.—FDP = flat-panel detector.

Aspects of Image Quality

Table 2 shows some relevant technical features of various radiography systems.

Pixel Size, Matrix, and Detector Size

Digital images consist of picture elements, or pixels. The two-dimensional collection of pixels in the image is called the matrix, which is usually expressed as length (in pixels) by width (in pixels) (Table 2). Maximum achievable spatial resolution (Nyquist frequency, given in cycles per milli-

meter) is defined by pixel size and spacing. The smaller the pixel size (or the larger the matrix), the higher the maximum achievable spatial resolution.

The overall detector size determines if the detector is suitable for all clinical applications. Larger detector areas are needed for chest imaging than for imaging of the extremities. In cassette-based systems, different sizes are available.

Spatial Resolution

Spatial resolution refers to the minimum resolvable separation between high-contrast objects. In digital detectors, spatial resolution is defined and limited by the minimum pixel size. Increasing the radiation applied to the detector will not improve the maximum spatial resolution. On the other hand, scatter of x-ray quanta and light photons within the detector influences spatial resolution. Therefore, the intrinsic spatial resolution for selenium-based direct conversion detectors is higher than that for indirect conversion detectors. Structured scintillators offer advantages over unstructured scintillators.

According to the Nyquist theorem, given a pixel size a , the maximum achievable spatial resolution is $a/2$. At a pixel size of 200 μm , the maximum detectable spatial frequency will be 2.5 cycles/mm. The diagnostic range for general radiography is 0–3 cycles/mm (34,54); only older generations of storage phosphors do not meet this criterion (Table 2). For digital mammography, the demanded diagnostic spatial resolution is substantially higher (>5 cycles/mm), indicating the need for specially designed dedicated detectors with smaller pixel sizes and higher resolutions (11).

Modulation Transfer Function

Modulation transfer function (MTF) is the capacity of the detector to transfer the modulation of the input signal at a given spatial frequency to its output (55). At radiography, objects having different sizes and opacity are displayed with different gray-scale values in an image. MTF has to do with the display of contrast and object size. More specifically, MTF is responsible for converting contrast values of different-sized objects (object contrast) into contrast intensity levels in the image (image contrast). For general imaging, the relevant details are in a range between 0 and 2 cycles/mm, which demands high MTF values.

MTF is a useful measure of true or effective resolution, since it accounts for the amount of blur and contrast over a range of spatial frequencies. MTF values of various detectors were measured and further discussed by Illers et al (56).

Dynamic Range

Dynamic range is a measure of the signal response of a detector that is exposed to x-rays (55). In conventional screen-film combinations, the dynamic range gradation curve is S shaped within a narrow exposure range for optimal film blackening (Fig 8); thus, the film has a low tolerance for an exposure that is higher or lower than required, resulting in failed exposures or insufficient image

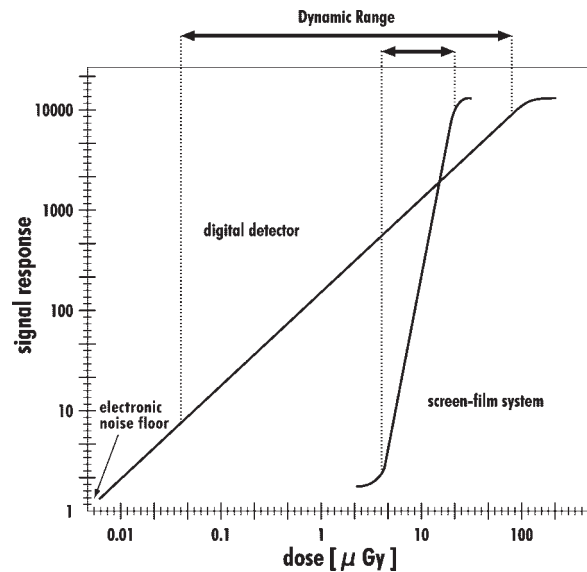


Figure 8. Graph illustrates the dynamic range of screen-film combinations and digital detectors. Screen-film systems have only a limited tolerance for radiation exposure, resulting in a steep and tight curve, whereas the curve for digital detectors is less steep and covers a wider range. As a result, an optimal signal response will occur over a wider exposure range with digital detectors than with screen-film combinations.

quality. For digital detectors, dynamic range is the range of x-ray exposure over which a meaningful image can be obtained. Digital detectors have a wider and linear dynamic range, which, in clinical practice, virtually eliminates the risk of a failed exposure. Another positive effect of a wide dynamic range is that differences between specific tissue absorptions (eg, bone vs soft tissue) can be displayed in one image without the need for additional images. On the other hand, because detector function improves as radiation exposure increases, special care has to be taken not to overexpose the patient by applying more radiation than is needed for a diagnostically sufficient image.

Detective Quantum Efficiency

Detective quantum efficiency (DQE) is one of the fundamental physical variables related to image quality in radiography and refers to the efficiency of a detector in converting incident x-ray energy into an image signal. DQE is calculated by comparing the signal-to-noise ratio at the detector output with that at the detector input as a function of spatial frequency (55). DQE is dependent on radiation exposure, spatial frequency, MTF, and detector material. The quality (voltage and current) of the radiation applied is also an important influence on DQE (41).

High DQE values indicate that less radiation is needed to achieve identical image quality; increasing the DQE and leaving radiation exposure constant will improve image quality.

Teaching Point

Teaching Point

Teaching Point

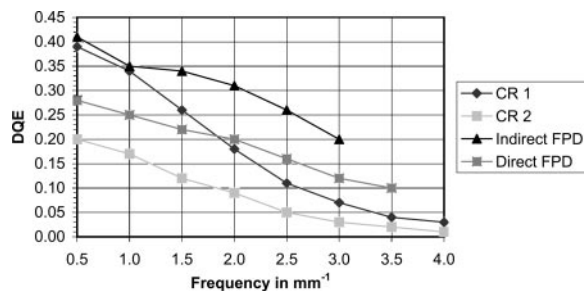


Figure 9. Graph illustrates the DQE curves for four digital detectors. *CR 1* = needle-structured storage phosphor and line scanner (MD5.0/DX-S; Agfa-Gevaert, Mortsel, Belgium), *CR 2* = unstructured storage phosphor and flying-spot scanner (MD40/ADC Compact, Agfa-Gevaert), *Indirect FPD* = CsI-based flat-panel detector (Pixium 4600; Trixell, Moirans, France), *Direct FPD* = selenium-based flat-panel detector (DR 9000; Kodak, Rochester, NY).

The ideal detector would have a DQE of 1, meaning that all the radiation energy is absorbed and converted into image information. In practice, the DQE of digital detectors is limited to about 0.45 at 0.5 cycles/mm (Fig 9). During the past few years, various methods of measuring DQE have been established (41), making the comparison of DQE values difficult if not impossible. In 2003, the IEC62220-1 standard was introduced to standardize DQE measurements and make them comparable.

The DQE curves for four different digital detectors are shown in Figure 9. Screen-film systems have a DQE comparable to that of detector CR 2 in Figure 9.

Radiation Exposure

In general, the higher DQE values of most digital detectors compared with screen-film combinations suggest that, besides providing better image quality, digital detectors have the potential for substantially lowering patient exposure without a loss of image quality. Efforts have been made to optimize both image quality and exposure in digital radiography.

The most obvious way to minimize patient exposure is to greatly reduce the number of failed exposures and requisite additional images. This reduction is made possible by the wider dynamic range of digital detectors compared with conventional screen-film combinations. Yet, this wider dynamic range will contribute little to reducing exposure to the individual patient. By reducing the amount of radiation exposure needed for a sufficient image, unnecessary exposure can be directly eliminated.

Only a few studies have investigated the possibility of reducing the exposure with storage-phosphor radiography. Heyne et al (57-59) published

three studies on exposure reduction in digital radiography of skull, hand, pelvis, and lumbar spine phantoms using a standard CR system. In all three studies, the authors concluded that reduction of exposure with storage-phosphor systems is possible to a variable extent, depending on the clinical problem and the specific clinical question. These results were confirmed by another trial, in which specimens of fractured wrists were used (60). Busch et al (61) compared various storage-phosphor systems with a flat-panel detector system at different exposures in radiography of low-contrast, hand, abdomen, and chest phantoms. The authors found that exposure reduction with storage-phosphor systems is limited to certain clinical indications and cannot be applied unrestrictedly in clinical practice because some incidental finding might be masked by increased image noise in low-exposure images (61). Reasonable exposure reduction requires settings in which the chance of underdiagnosis is minimized.

Unlike storage-phosphor systems, in which the possibility of exposure reduction is limited, DR systems offer a significantly higher potential for general exposure reduction because of their far superior quantum efficiency. Several studies have shown that a considerably lower exposure is required for equivalent depiction of anatomic details with flat-panel detectors than with storage-phosphor systems and screen-film combinations for different clinical fields, including radiography of the extremities and chest (16,17,22-25,27,32,35,37,40,43,45,47,49,51,52,62-65). In most of these studies, indirect conversion flat-panel detectors showed the highest potential for reducing exposure, regardless of the clinical setting. There have also been numerous studies comparing various digital detectors within the same application (16,17). The authors of these studies also concluded that flat-panel detectors achieved the best results in low-exposure imaging, followed by other DR systems such as selenium drum- and CCD-based systems.

Although almost all of these studies agree as to the ranking of the systems in terms of the degree of exposure reduction, the total percentage of suggested reduction varies dramatically (64). Consequently, requirements for the optimization of image quality may differ even within the departments that conducted the studies, and general recommendations for optimal imaging exposures for specific indications cannot be given. In summary, reduction of exposure in flat-panel detector digital radiography is possible, to some extent regardless of the clinical situation.

Reports of an increase of exposure with digital radiography are rare and concern only chest radiography with storage phosphors (66,67). One reason for these apparently contradictory findings is the effectively variable speed of CR systems and the willingness of radiologists to accept more noise in some of the images obtained with these systems (66). Another reason might be that both studies were published in 2000, having made use of somewhat older generations of storage phosphors and scanners.

A study by Geijer et al (68) and one by Geijer alone (69) described an increase of exposure in the imaging of scoliosis with a direct conversion flat-panel detector. However, this finding was put into perspective by the fact that optimization of the DR systems yielded superior image quality at lower exposure (69).

Future Technologies and Perspectives

New storage phosphors and scanning systems are being investigated for use in CR. These phosphors are structured, since their crystals are grown in a needle shape, and are coated on a glass or aluminum substrate without any binding material between the crystals (70,71). This technique offers tighter phosphor packing and reduced pixel size, resulting in DQE values that are as high as those for indirect conversion flat-panel detector systems (Fig 9) (70,72,73). In addition, images are scanned line by line with this system, resulting in shorter scanning times. Line scanners could also read out each pixel of a line for a longer time if scanning time is kept constant compared with that of a flying-spot scanner, which results in a higher signal being produced by the emitted light. Initial clinical studies in chest radiography with this system have shown equal quality with a state-of-the-art unstructured CR system with the exposure lowered to 50% (72).

With the introduction of portable devices, flat-panel detector systems will be more flexible and might even replace CR systems (8,42,43). However, the image quality afforded by these portable devices must be further investigated and compared with that afforded by storage-phosphor systems.

Another promising application is the use of dynamic flat-panel detectors in fluoroscopy (9,55). Studies using these systems have indicated improved image quality and reduced patient exposure (74,75), although there are also reports that do not indicate reduced exposure (76).

Improvement in the DQE and signal-to-noise ratio of detectors may lead to even further reduc-

tion of exposure or improvement in image quality. The architecture of the readout arrays could be optimized by reducing the size of the circuit and pixels.

Conclusions

The future of radiography will be digital. The advantages of digital radiography with respect to various imaging systems have been extensively discussed in the literature. The large number of scientific papers dealing with digital radiography that have been published over the last 25 years also indicates the importance of this topic to the radiologist.

References

1. Kruger RA, Mistretta CA, Crummy AB, et al. Digital K-edge subtraction radiography. *Radiology* 1977;125:243-245.
2. Ovitt TW, Christenson PC, Fisher HD 3rd, et al. Intravenous angiography using digital video subtraction: x-ray imaging system. *AJR Am J Roentgenol* 1980;135:1141-1144.
3. Moore R. Computed radiography. *Med Electron* 1980;11:78-79.
4. Neitzel U, Maack I, Gunther-Kohfahl S. Image quality of a digital chest radiography system based on a selenium detector. *Med Phys* 1994;21:509-516.
5. Antonuk LE, Yorkston J, Huang W, et al. A real-time, flat-panel, amorphous silicon, digital x-ray imager. *RadioGraphics* 1995;15:993-1000.
6. Zhao W, Rowlands JA. X-ray imaging using amorphous selenium: feasibility of a flat panel self-scanned detector for digital radiology. *Med Phys* 1995;22:1595-1604.
7. Kandarakis I, Cavouras D, Panayiotakis GS, et al. Evaluating x-ray detectors for radiographic applications: a comparison of ZnSCdS:Ag with Gd₂O₂S:Tb and Y₂O₂S:Tb screens. *Phys Med Biol* 1997;42:1351-1373.
8. Puig S. Digital radiography of the chest in pediatric patients [in German]. *Radiologe* 2003;43:1045-1050.
9. Choquette M, Demers Y, Shukri Z, et al. Performance of a real-time selenium-based x-ray detector for fluoroscopy. *Proc SPIE* 2001;4320:501-508.
10. Colbeth R, Boyce S, Fong R, et al. 40 × 30 cm flat-panel imager for angiography, R&F, and cone-beam CT applications. *Proc SPIE* 2001;4320:94-102.
11. Mahesh M. AAPM/RSNA physics tutorial for residents. Digital mammography: an overview. *RadioGraphics* 2004;24:1747-1760.
12. Rowlands JA. The physics of computed radiography. *Phys Med Biol* 2002;47:R123-R166.
13. Bernhardt TM, Otto D, Reichel G, et al. Detection of simulated interstitial lung disease and catheters with selenium, storage phosphor, and film-based radiography. *Radiology* 1999;213:445-454.
14. Kirchner J, Stueckle CA, Schilling EM, et al. Efficacy of daily bedside chest radiography as visualized by digital luminescence radiography. *Australas Radiol* 2001;45:444-447.
15. Schaefer-Prokop CM, Prokop M. Storage phosphor radiography. *Eur Radiol* 1997;7:58-65.

16. Veldkamp WJ, Kroft LJ, Boot MV, et al. Contrast-detail evaluation and dose assessment of eight digital chest radiography systems in clinical practice. *Eur Radiol* 2006;16:333–341.
17. Kroft LJ, Veldkamp WJ, Mertens BJ, et al. Comparison of eight different digital chest radiography systems: variation in detection of simulated chest disease. *AJR Am J Roentgenol* 2005;185:339–346.
18. Ono K, Yoshitake T, Akahane K, et al. Comparison of a digital flat-panel versus screen-film, photo-fluorography and storage-phosphor systems by detection of simulated lung adenocarcinoma lesions using hard copy images. *Br J Radiol* 2005;78:922–927.
19. Uffmann M, Prokop M, Eisenhuber E, et al. Computed radiography and direct radiography: influence of acquisition dose on the detection of simulated lung lesions. *Invest Radiol* 2005;40:249–256.
20. Uffmann M, Schaefer-Prokop C, Neitzel U, et al. Skeletal applications for flat-panel versus storage-phosphor radiography: effect of exposure on detection of low-contrast details. *Radiology* 2004;231:506–514.
21. Ganten M, Radeleff B, Kampschulte A, et al. Comparing image quality of flat-panel chest radiography with storage phosphor radiography and film-screen radiography. *AJR Am J Roentgenol* 2003;181:171–176.
22. Ludwig K, Henschel A, Bernhardt TM, et al. Performance of a flat-panel detector in the detection of artificial erosive changes: comparison with conventional screen-film and storage-phosphor radiography. *Eur Radiol* 2003;13:1316–1323.
23. Fischbach F, Ricke J, Freund T, et al. Flat panel digital radiography compared with storage phosphor computed radiography: assessment of dose versus image quality in phantom studies. *Invest Radiol* 2002;37:609–614.
24. Herrmann A, Bonel H, Stabler A, et al. Chest imaging with flat-panel detector at low and standard doses: comparison with storage phosphor technology in normal patients. *Eur Radiol* 2002;12:385–390.
25. Ludwig K, Lenzen H, Kamm KF, et al. Performance of a flat-panel detector in detecting artificial bone lesions: comparison with conventional screen-film and storage-phosphor radiography. *Radiology* 2002;222:453–459.
26. Goo JM, Im JG, Lee HJ, et al. Detection of simulated chest lesions by using soft-copy reading: comparison of an amorphous silicon flat-panel-detector system and a storage-phosphor system. *Radiology* 2002;224:242–246.
27. Kim TS, Im JG, Goo JM, et al. Detection of pulmonary edema in pigs: storage phosphor versus amorphous selenium-based flat-panel-detector radiography. *Radiology* 2002;223:695–701.
28. Rong XJ, Shaw CC, Liu X, et al. Comparison of an amorphous silicon/cesium iodide flat-panel digital chest radiography system with screen/film and computed radiography systems: a contrast-detail phantom study. *Med Phys* 2001;28:2328–2335.
29. Goo JM, Im JG, Kim JH, et al. Digital chest radiography with a selenium-based flat-panel detector versus a storage phosphor system: comparison of soft-copy images. *AJR Am J Roentgenol* 2000;175:1013–1018.
30. Yaffe MJ, Rowlands JA. X-ray detectors for digital radiography. *Phys Med Biol* 1997;42:1–39.
31. Fischbach F, Freund T, Pech M, et al. Comparison of indirect CsI/a:Si and direct a:Se digital radiography: an assessment of contrast and detail visualization. *Acta Radiol* 2003;44:616–621.
32. Ramli K, Abdullah BJ, Ng KH, et al. Computed and conventional chest radiography: a comparison of image quality and radiation dose. *Australas Radiol* 2005;49:460–466.
33. Zhao W, Ji WG, Debie A, et al. Imaging performance of amorphous selenium based flat-panel detectors for digital mammography: characterization of a small area prototype detector. *Med Phys* 2003;30:254–263.
34. Chotas HG, Dobbins JT 3rd, Ravin CE. Principles of digital radiography with large-area, electronically readable detectors: a review of the basics. *Radiology* 1999;210:595–599.
35. Kroft LJ, Geleijns J, Mertens BJ, et al. Digital slot-scan charge-coupled device radiography versus AMBER and Bucky screen-film radiography for detection of simulated nodules and interstitial disease in a chest phantom. *Radiology* 2004;231:156–163.
36. Veldkamp WJ, Kroft LJ, Mertens BJ, et al. Digital slot-scan charge-coupled device radiography versus AMBER and Bucky screen-film radiography: comparison of image quality in a phantom study. *Radiology* 2005;235:857–866.
37. Pascoal A, Lawinski CP, Mackenzie A, et al. Chest radiography: a comparison of image quality and effective dose using four digital systems. *Radiat Prot Dosimetry* 2005;114:273–277.
38. Noel A, Thibault F. Digital detectors for mammography: the technical challenges. *Eur Radiol* 2004;14:1990–1998.
39. Kotter E, Langer M. Digital radiography with large-area flat-panel detectors. *Eur Radiol* 2002;12:2562–2570.
40. Strotzer M, Gmeinwieser J, Volk M, et al. Clinical application of a flat-panel X-ray detector based on amorphous silicon technology: image quality and potential for radiation dose reduction in skeletal radiography. *AJR Am J Roentgenol* 1998;171:23–27.
41. Illers H, Buhr E, Hoeschen C. Measurement of the detective quantum efficiency (DQE) of digital X-ray detectors according to the novel standard IEC 62220–1. *Radiat Prot Dosimetry* 2005;114:39–44.
42. Rapp-Bernhardt U, Bernhardt TM, Lenzen H, et al. Experimental evaluation of a portable indirect flat-panel detector for the pediatric chest: comparison with storage phosphor radiography at different exposures by using a chest phantom. *Radiology* 2005;237:485–491.
43. Rapp-Bernhardt U, Roehl FW, Esseling R, et al. Portable flat-panel detector for low-dose imaging in a pediatric intensive care unit: comparison with an asymmetric film-screen system. *Invest Radiol* 2005;40:736–741.
44. Chotas HG, Ravin CE. Digital chest radiography with a solid-state flat-panel x-ray detector: contrast-detail evaluation with processed images printed on film hard copy. *Radiology* 2001;218:679–682.

45. Fink C, Hallscheidt PJ, Noeldge G, et al. Clinical comparative study with a large-area amorphous silicon flat-panel detector: image quality and visibility of anatomic structures on chest radiography. *AJR Am J Roentgenol* 2002;178:481-486.
46. Floyd CE Jr, Warp RJ, Dobbins JT 3rd, et al. Imaging characteristics of an amorphous silicon flat-panel detector for digital chest radiography. *Radiology* 2001;218:683-688.
47. Geijer H, Beckman KW, Andersson T, et al. Image quality vs. radiation dose for a flat-panel amorphous silicon detector: a phantom study. *Eur Radiol* 2001;11:1704-1709.
48. Okamura T, Tanaka S, Koyama K, et al. Clinical evaluation of digital radiography based on a large-area cesium iodide-amorphous silicon flat-panel detector compared with screen-film radiography for skeletal system and abdomen. *Eur Radiol* 2002;12:1741-1747.
49. Strotzer M, Volk M, Reiser M, et al. Chest radiography with a large-area detector based on cesium-iodide/amorphous-silicon technology: image quality and dose requirement in comparison with an asymmetric screen-film system. *J Thorac Imaging* 2000;15:157-161.
50. Strotzer M, Volk M, Wild T, et al. Simulated bone erosions in a hand phantom: detection with conventional screen-film technology versus cesium iodide-amorphous silicon flat-panel detector. *Radiology* 2000;215:512-515.
51. Volk M, Strotzer M, Holzknacht N, et al. Digital radiography of the skeleton using a large-area detector based on amorphous silicon technology: image quality and potential for dose reduction in comparison with screen-film radiography. *Clin Radiol* 2000;55:615-621.
52. Bacher K, Smeets P, Bonnarens K, et al. Dose reduction in patients undergoing chest imaging: digital amorphous silicon flat-panel detector radiography versus conventional film-screen radiography and phosphor-based computed radiography. *AJR Am J Roentgenol* 2003;181:923-929.
53. Prokop M, Schaefer-Prokop CM. Digital image processing. *Eur Radiol* 1997;7:73-82.
54. Neitzel U. Status and prospects of digital detector technology for CR and DR. *Radiat Prot Dosimetry* 2005;114:32-38.
55. Spahn M. Flat detectors and their clinical applications. *Eur Radiol* 2005;15:1934-1947.
56. Illers H, Buhler E, Gunther-Kohfahl S, et al. Measurement of the modulation transfer function of digital X-ray detectors with an opaque edge-test device. *Radiat Prot Dosimetry* 2005;114:214-219.
57. Heyne JP, Merbold H, Sehner J, et al. The reduction of the radiation dosage by means of storage phosphor-film radiography compared to a conventional film-screen system with a grid cassette on a skull phantom [in German]. *Rofo* 1999;171:54-59.
58. Heyne JP, Merbold H, Sehner J, et al. Reduction of radiation dosage by using digital luminescence radiography on a hand phantom [in German]. *Rofo* 2000;172:386-390.
59. Heyne JP, Sehner J, Neumann R, et al. Reduction of radiation exposure by using storage phosphor radiography on pelvis and lumbar spine [in German]. *Rofo* 2002;174:104-111.
60. Peer R, Lanser A, Giacomuzzi SM, et al. Storage phosphor radiography of wrist fractures: a subjective comparison of image quality at varying exposure levels. *Eur Radiol* 2002;12:1354-1359.
61. Busch HP, Busch S, Decker C, et al. Image quality and exposure dose in digital projection radiography. *Rofo* 2003;175:32-37.
62. Strotzer M, Volk M, Frund R, et al. Routine chest radiography using a flat-panel detector: image quality at standard detector dose and 33% dose reduction. *AJR Am J Roentgenol* 2002;178:169-171.
63. Hosch WP, Fink C, Radeleff B, et al. Radiation dose reduction in chest radiography using a flat-panel amorphous silicon detector. *Clin Radiol* 2002;57:902-907.
64. Neofotistou V, Tsapaki V, Kottou S, Schreiner-Karoussou A, Vano E. Does digital imaging decrease patient dose? a pilot study and review of the literature. *Radiat Prot Dosimetry* 2005;117:204-210.
65. Volk M, Strotzer M, Gmeinwieser J, et al. Flat-panel x-ray detector using amorphous silicon technology: reduced radiation dose for the detection of foreign bodies. *Invest Radiol* 1997;32:373-377.
66. Heggie JC, Wilkinson LE. Radiation doses from common radiographic procedures: a ten year perspective. *Australas Phys Eng Sci Med* 2000;23:124-134.
67. Weatherburn GC, Bryan S, Davies JG. Comparison of doses for bedside examinations of the chest with conventional screen-film and computed radiography: results of a randomized controlled trial. *Radiology* 2000;217:707-712.
68. Geijer H, Beckman K, Jonsson B, et al. Digital radiography of scoliosis with a scanning method: initial evaluation. *Radiology* 2001;218:402-410.
69. Geijer H. Radiation dose and image quality in diagnostic radiology: optimization of the dose-image quality relationship with clinical experience from scoliosis radiography, coronary intervention and a flat-panel digital detector. *Acta Radiol Suppl* 2002;43:1-43.
70. Leblans P, Struye L, Willems P. A new needle-crystalline computed radiography detector. *J Digit Imaging* 2000;13:117-120.
71. Schillinger B, Baumann J, Gebele H, et al. A new fast and large area neutron detector using a novel image plate readout technique. *Appl Radiat Isot* 2004;61:451-454.
72. Korner M, Wirth S, Treitl M, et al. Initial clinical results with a new needle screen storage phosphor system in chest radiograms. *Rofo* 2005;177:1491-1496.
73. Frankenberger J, Mair S, Herrmann C, Lamotte J, Fasbender R. Reflective and transmissive CR ScanHead technology on needle image plates. *Proc SPIE* 2005;5745:499-510.
74. Suzuki S, Furui S, Kobayashi I, et al. Radiation dose to patients and radiologists during transcatheter arterial embolization: comparison of a digital flat-panel system and conventional unit. *AJR Am J Roentgenol* 2005;185:855-859.
75. Vano E, Geiger B, Schreiner A, et al. Dynamic flat panel detector versus image intensifier in cardiac imaging: dose and image quality. *Phys Med Biol* 2005;50:5731-5742.
76. Trianni A, Bernardi G, Padovani R. Are new technologies always reducing patient doses in cardiac procedures? *Radiat Prot Dosimetry* 2005;117:97-101.

Advances in Digital Radiography: Physical Principles and System Overview

Markus Körner, MD et al

RadioGraphics 2007; 27:675–686 • Published online 10.1148/rg.273065075 • Content Code: PH

Page 676

CR systems use storage-phosphor image plates with a separate image readout process; DR is a way of converting x-rays into electrical charges by means of a direct readout process. DR systems can be further divided into direct and indirect conversion groups depending on the type of x-ray conversion used.

Page 680

Image processing is one of the key features of digital radiography, greatly influencing the way the image appears to the radiologist (53).

Page 682

Spatial resolution refers to the minimum resolvable separation between high-contrast objects. In digital detectors, spatial resolution is defined and limited by the minimum pixel size.

Page 682

Dynamic range is a measure of the signal response of a detector that is exposed to x-rays (55).

Page 682

Detective quantum efficiency (DQE) is one of the fundamental physical variables related to image quality in radiography and refers to the efficiency of a detector in converting incident x-ray energy into an image signal.

RadioGraphics 2007

This is your reprint order form or pro forma invoice

(Please keep a copy of this document for your records.)

Reprint order forms and purchase orders or prepayments must be received 72 hours after receipt of form either by mail or by fax at 410-820-9765. It is the policy of Cadmus Reprints to issue one invoice per order.

Please print clearly.

Author Name _____
Title of Article _____
Issue of Journal _____ Reprint # _____ Publication Date _____
Number of Pages _____ KB # _____ Symbol RadioGraphics
Color in Article? Yes / No (Please Circle)

Please include the journal name and reprint number or manuscript number on your purchase order or other correspondence.

Order and Shipping Information

Reprint Costs (Please see page 2 of 2 for reprint costs/fees.)

_____ Number of reprints ordered \$ _____
_____ Number of color reprints ordered \$ _____
_____ Number of covers ordered \$ _____
Subtotal \$ _____
Taxes \$ _____

(Add appropriate sales tax for Virginia, Maryland, Pennsylvania, and the District of Columbia or Canadian GST to the reprints if your order is to be shipped to these locations.)

First address included, add \$32 for
each additional shipping address \$ _____

TOTAL \$ _____

Shipping Address (cannot ship to a P.O. Box) Please Print Clearly

Name _____
Institution _____
Street _____
City _____ State _____ Zip _____
Country _____
Quantity _____ Fax _____
Phone: Day _____ Evening _____
E-mail Address _____

Additional Shipping Address* (cannot ship to a P.O. Box)

Name _____
Institution _____
Street _____
City _____ State _____ Zip _____
Country _____
Quantity _____ Fax _____
Phone: Day _____ Evening _____
E-mail Address _____

* Add \$32 for each additional shipping address

Payment and Credit Card Details

Enclosed: Personal Check _____
Credit Card Payment Details _____
Checks must be paid in U.S. dollars and drawn on a U.S. Bank.
Credit Card: __ VISA __ Am. Exp. __ MasterCard
Card Number _____
Expiration Date _____
Signature: _____

Please send your order form and prepayment made payable to:

Cadmus Reprints
P.O. Box 751903
Charlotte, NC 28275-1903

Note: Do not send express packages to this location, PO Box.
FEIN #: 541274108

Signature _____ Date _____

Signature is required. By signing this form, the author agrees to accept the responsibility for the payment of reprints and/or all charges described in this document.

Invoice or Credit Card Information

Invoice Address Please Print Clearly

Please complete Invoice address as it appears on credit card statement

Name _____
Institution _____
Department _____
Street _____
City _____ State _____ Zip _____
Country _____
Phone _____ Fax _____
E-mail Address _____

Cadmus will process credit cards and Cadmus Journal Services will appear on the credit card statement.

If you don't mail your order form, you may fax it to 410-820-9765 with your credit card information.

RadioGraphics 2007

Black and White Reprint Prices

Domestic (USA only)						
# of Pages	50	100	200	300	400	500
1-4	\$213	\$228	\$260	\$278	\$295	\$313
5-8	\$338	\$373	\$420	\$453	\$495	\$530
9-12	\$450	\$500	\$575	\$635	\$693	\$755
13-16	\$555	\$623	\$728	\$805	\$888	\$965
17-20	\$673	\$753	\$883	\$990	\$1,085	\$1,185
21-24	\$785	\$880	\$1,040	\$1,165	\$1,285	\$1,413
25-28	\$895	\$1,010	\$1,208	\$1,350	\$1,498	\$1,638
29-32	\$1,008	\$1,143	\$1,363	\$1,525	\$1,698	\$1,865
Covers	\$95	\$118	\$218	\$320	\$428	\$530

Color Reprint Prices

Domestic (USA only)						
# of Pages	50	100	200	300	400	500
1-4	\$218	\$233	\$343	\$460	\$579	\$697
5-8	\$343	\$388	\$584	\$825	\$1,069	\$1,311
9-12	\$471	\$503	\$828	\$1,196	\$1,563	\$1,935
13-16	\$601	\$633	\$1,073	\$1,562	\$2,058	\$2,547
17-20	\$738	\$767	\$1,319	\$1,940	\$2,550	\$3,164
21-24	\$872	\$899	\$1,564	\$2,308	\$3,045	\$3,790
25-28	\$1,004	\$1,035	\$1,820	\$2,678	\$3,545	\$4,403
29-32	\$1,140	\$1,173	\$2,063	\$3,048	\$4,040	\$5,028
Covers	\$95	\$118	\$218	\$320	\$428	\$530

International (includes Canada and Mexico)						
# of Pages	50	100	200	300	400	500
1-4	\$263	\$275	\$330	\$385	\$430	\$485
5-8	\$415	\$443	\$555	\$650	\$753	\$850
9-12	\$563	\$608	\$773	\$930	\$1,070	\$1,228
13-16	\$698	\$760	\$988	\$1,185	\$1,388	\$1,585
17-20	\$848	\$925	\$1,203	\$1,463	\$1,705	\$1,950
21-24	\$985	\$1,080	\$1,420	\$1,725	\$2,025	\$2,325
25-28	\$1,135	\$1,248	\$1,640	\$1,990	\$2,350	\$2,698
29-32	\$1,273	\$1,403	\$1,863	\$2,265	\$2,673	\$3,075
Covers	\$148	\$168	\$308	\$463	\$615	\$768

International (includes Canada and Mexico)						
# of Pages	50	100	200	300	400	500
1-4	\$268	\$280	\$412	\$568	\$715	\$871
5-8	\$419	\$457	\$720	\$1,022	\$1,328	\$1,633
9-12	\$583	\$610	\$1,025	\$1,492	\$1,941	\$2,407
13-16	\$742	\$770	\$1,333	\$1,943	\$2,556	\$3,167
17-20	\$913	\$941	\$1,641	\$2,412	\$3,169	\$3,929
21-24	\$1,072	\$1,100	\$1,946	\$2,867	\$3,785	\$4,703
25-28	\$1,246	\$1,274	\$2,254	\$3,318	\$4,398	\$5,463
29-32	\$1,405	\$1,433	\$2,561	\$3,788	\$5,014	\$6,237
Covers	\$148	\$168	\$308	\$463	\$615	\$768

Minimum order is 50 copies. For orders larger than 500 copies, please consult Cadmus Reprints at 800-407-9190.

Reprint Cover

Cover prices are listed above. The cover will include the publication title, article title, and author name in black.

Shipping

Shipping costs are included in the reprint prices. Domestic orders are shipped via UPS Ground service. Foreign orders are shipped via a proof of delivery air service.

Multiple Shipments

Orders can be shipped to more than one location. Please be aware that it will cost \$32 for each additional location.

Delivery

Your order will be shipped within 2 weeks of the journal print date. Allow extra time for delivery.

Tax Due

Residents of Virginia, Maryland, Pennsylvania, and the District of Columbia are required to add the appropriate sales tax to each reprint order. For orders shipped to Canada, please add 7% Canadian GST unless exemption is claimed.

Ordering

Reprint order forms and purchase order or prepayment is required to process your order. Please reference journal name and reprint number or manuscript number on any correspondence. You may use the reverse side of this form as a proforma invoice. Please return your order form and prepayment to:

Cadmus Reprints

P.O. Box 751903
Charlotte, NC 28275-1903

Note: Do not send express packages to this location, PO Box.
FEIN #: 541274108

Please direct all inquiries to:

Rose A. Baynard

800-407-9190 (toll free number)
410-819-3966 (direct number)
410-820-9765 (FAX number)
baynardr@cadmus.com (e-mail)

Reprint Order Forms and purchase order or prepayments must be received 72 hours after receipt of form.